International Journal of Fluid Machinery and Systems
Vol. 14, No. 4, October-December 2021
DOI: http://dx.doi.org/10.5293/IJFMS.2021.14.4.335
ISSN (Online): 1882-9554

Original Paper

Numerical Investigation on a Twin-Screw Multiphase Pump Under low IGVF

Shuaihui Sun[1], Pengbo Wu[1], Pengcheng Guo[1], Guangzhi Yi[1] and Ahmed Kovacevic[2]

[1]State Key Laboratory of Eco-hydraulics in Northwest Arid Region,
Xi'an University of Technology, Xi'an, 710048, China
[2]Centre for Compressor Technology, City, University of London,
London, EC1V 0HB, UK

Abstract

A three-dimensional transient numerical model was developed to obtain the two-phase flow characteristics in a twin-screw multiphase pump based on dynamic mesh technology and the multiphase flow model. The pump performance under different inlet gas volume fractions (IGVF) was predicted by the numerical model and was tested. Then, the numerical model was validated after comparing the simulation and experimental results. After that, the flow field in the pump under 10% IGVF was analyzed. When the IGVF is 10%, the pressure increases step by step and is symmetrical from both ends to the middle of the screw rotors. The pressure distribution through a single working chamber is uniform. It falls rapidly at the inlet of the tooth tip gap and then drops linearly in the gap channel. At the outlet of the tip gap, the pressure temporarily falls due to the high-speed jet. The GVF distribution in the working chamber is uneven. The leakage flow is laminar in the tip gap, and the liquid concentrates on the top of the gap. When the last working chamber connects with the discharge chamber, the discharge jet flow causes the vortices in the discharge pipe. The gas gradually moves to the center of the vortices, forming four gas-phase aggregation regions. The velocity of the interlobe leakage is the largest. The maximum velocity appears at the second cross-section and reaches 35m/s. This research can be used to improve the performance of the twin-screw multiphase pump under two-phase working conditions.

Keywords: Twin-screw multiphase pump, dynamic mesh, flow field, Leakage flow, two-phase flow

1. Introduction

In the conventional oil and gas delivery system, gas needs to be separated from oil and water by separators firstly. Then the gas and liquid are transported by the compressors and pumps, which leads to extensive investment and high operation costs. Multiphase transportation technology takes significant advantages over the separation phase transportation in oil-gas exploration, such as low cost, high production, and improving life expectancy, especially in the deep-sea oil-gas production system [1]. The twin-screw multiphase pumps are the critical equipment in the multiphase transportation system [2,3]. They can transport high viscosity or high IGVF fluid and handle the drastic change of working conditions. However, the twin-screw multiphase pumps have less efficiency and lower stability than the centrifugal pump. In order to improve its multiphase transport efficiency and operational stability, researchers have conducted a series of research work from theoretical simulation and experiments. Vetter et al. [4] proposed a one-dimensional theoretical model for predicting the performance of a twin-screw multiphase pump, which considered the working process of the pump as a series of moving cylinders that were moving from the entrance to the outlet. The cylinders were connected with the tip gap. Therefore, the liquid was pushed toward the tip of the rotors by centrifugal force, and the leakage flow rate can be considered as pure-liquid leakage [5]. Cao et al. [6,7] proposed a chamber model and verified it with experimental results. In the model, the volume of the suction chamber and the discharge chamber varied with the rotational angle, while the working chamber volume was kept unchanged. The leakage flow at the tip gap was assumed to be single-phase, and that at the flank gap was assumed to be two-phase. K. Rabiger[8] developed a chamber model for predicting the performance of a twin-screw multiphase pump under high IGVF (90%~99%) conditions and validated it with the high-speed camera test. Zhang[9] used the parallel plate theory to deduce the leakage calculation equation for pure-liquid leakage in a twin-screw pump. Using the two-phase homogeneous leakage equations, LIU[10] and SHIV[11] calculated the leakage flow in a twin-screw multiphase pump. Yan[12] studied the influence of IGVF on a multiphase centrifugal pump's performance and indicated that the direction of the impeller radial force varied with the change of IGVF. However, due to the difference between the actual flow and the leakage model assumption, the prediction accuracy of the chamber model was determined by the flow coefficient of

Received July 16 2021; accepted for publication September 9 2021:
Review conducted by Xuelin Tang. (Paper number O21036J) Corresponding author: Pengcheng Guo, guoyicheng@xaut.edu.cn

the leakage equation and was low.

CFD technology provides new methods for obtaining the performance and internal flow field of the twin-screw multiphase pump. Due to the movement and deformation of the twin-screw pump chambers, dynamic mesh technology was required to calculate the transient flow field in the twin-screw multiphase pump. Kovacevic[13, 14] has developed the dynamic mesh generation software SCORG for twin-screw machines. Yan[15-17] generated the single-domain grids for a screw pump using the SCORG and calculated the transient flow field of the twin-screw pump. The influence of the screw rotor profile on the pump's performance and the transient flow field was analyzed. Zhang[18] calculated the pressure distribution in a double-suction twin-screw pump and analyzed the leakage flow in the pump. The hydraulic characteristics of a twin-screw pump were investigated f by the transient simulation based on the SCORG and Pumplinx[19]. Zhang[20] proposed a design method of multi-gradient variable pitch screw pump to improve the volumetric efficiency and solve the vibration problems under wet gas conditions. Sun[21] studied the gas-phase distribution on the rotor surface and in the working chamber of a twin-screw multiphase pump under different IGVF conditions. Zhang[22] used an immersed solid method coupled with CFD simulations to simulate the internal flow field of a double helix pump. The simulation model was validated with the experimental results, and some specific local flow characteristics were obtained. The results pointed out that the tip leakage occupied the main part of the total leakage. Little literature studied the twin-screw multiphase pump using the CFD method. The internal flow and leakage in twin-screw multiphase pumps are two-phase and more complicated than in twin-screw liquid pumps. The transportation and flow field characteristics under different IGVF are still unclear in twin-screw multiphase pumps.

Therefore, a transient numerical model for a twin-screw multiphase pump was developed in this paper based on dynamic mesh technology. The experiment was done to validate the model. The flow fields under low IGVF conditions were calculated out and analyzed. The transportation characteristics and the flow feature under 10% IGVF were analyzed. The results can eventually be used to improve the performance of the twin-screw multiphase pump.

2. Geometric model and numerical methods

2.1 Geometric models and basic parameters

Figure 1 is a structural diagram of a twin-screw multiphase pump. First, the fluid flows into the working chamber from the suction port in Fig. 1. Then the fluid pressure increases as the fluid is conveyed from the two ends to the middle of the pump. After that, the fluid flows out through the outlet, as shown in Fig. 2. The geometric parameters of a single screw rotor are shown in Table 1.

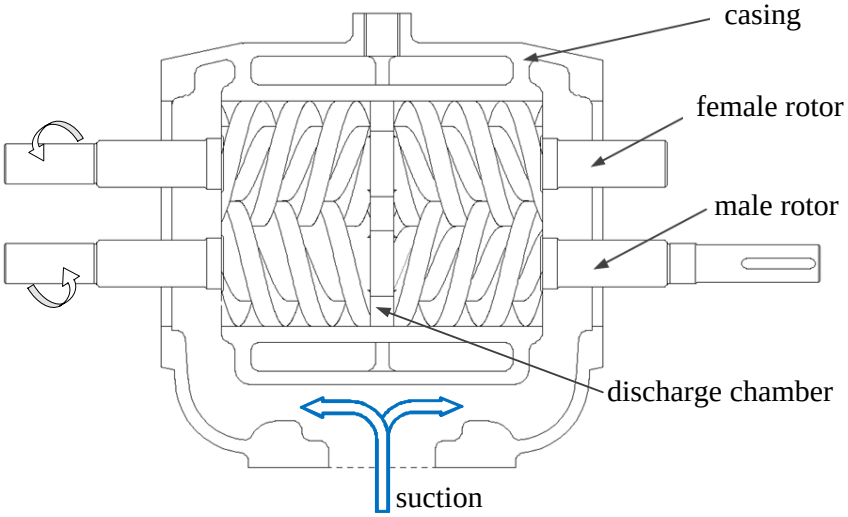

Fig. 1 Structure of the twin-screw multiphase pump

Table 1 Geometric parameters of a screw rotor

Parameters	Value
Tooth circle radius /mm	47
Tooth root radius /mm	28
Center distance /mm	75
Rotor length /mm	111
Tip gap /mm	0.1
Interlobe gap /mm	0.1
Theoretical volume /L	0.2664

2.2 Mesh Generation

The twin-screw multiphase pump is a positive displacement pump. ICEM was used to generate the unstructured mesh for the pump's inlet, outlet, and flow passage. They are static mesh and are shown in Fig. 2.

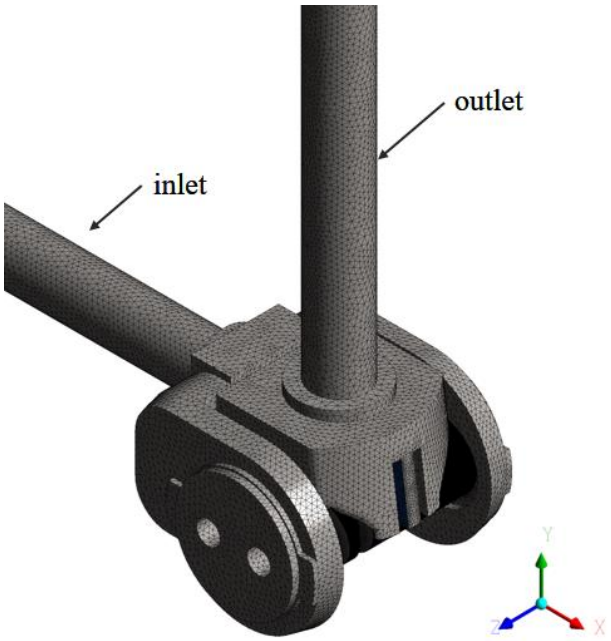

Fig. 2 Static Grids of twin-screw multiphase pump

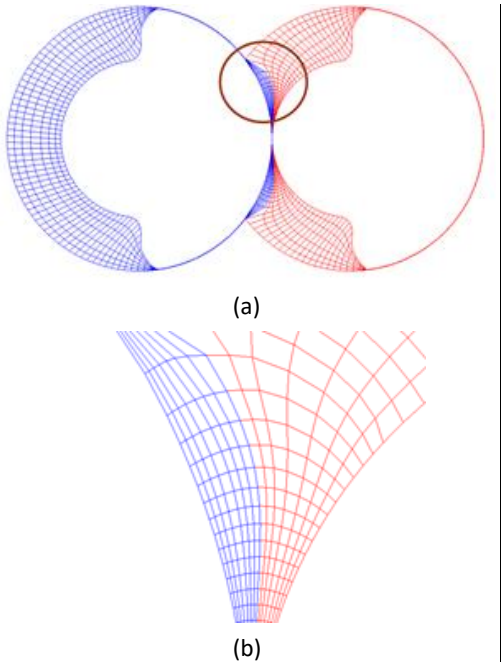

Fig. 3 Grids on the axial section in a working chamber

The rotor fluid domain rotates with the rotors. Therefore, dynamic mesh technology has to be used to capture the fluid domain's transient changes accurately. In addition, the size of the gap between male and female rotors is usually only one-thousandth of the diameter of the screw. Therefore, it is significant to generate enough grids for the gaps and the proper number of full grids simultaneously. In addition, The SCORG software [23] can generate the single fluid domain dynamic mesh for the screw rotor domain. Fig. 3(a) shows the mesh division of the axial section of the screw rotor using the rack line method, and Fig. 3(b) shows the partially enlarged view of the grids at the interlobe gap. The Circumferential divisions are applied on one interlobe segment of the full rotor profile. The Radial divisions are the number of meshes along the radial direction. The Interlobe divisions are the layers of the grids between each pitch of the rotor [24].

The grid independence verification is shown in Table 2. The number of grids in the rotor domain was increased by 1.33 times from Grids-1 to Grids-5. When the rotor grids increased from 1.764 million (Grids-4) to 2.347 million (Grids-5), the volumetric efficiency increased only 0.01%. Considering the number of grids and the calculation time comprehensively, Grids-4 was adopted as the calculation grids in the numerical simulation.

Table 2 Grid independence validation

	Number of rotor domain grids/million				The number of grids in the stationary domain /million	Total number of grids /million	volumetric efficiency /%
	Circumferential divisions	Radial divisions	Interlobe divisions	number of grids			
Grids-1	100	5	50	0.751	0.945	1.696	61.35
Grids-2	120	5	50	0.998		1.943	65.12
Grids-3	120	7	50	1.327		2.272	67.71
Grids-4	150	7	50	1.764		2.709	68.45
Grids-5	150	10	50	2.347		3.297	68.46

2.3 Boundary conditions and model settings

Water and air were working fluids in this paper. The IGVF is lower than 10% in this paper, and the gas can be assumed to be incompressible to simply the solution of the CFD model. Zhang[25] studied the bubble diameter at GVF 0%-50% and recommended that the bubble diameter was 0.2mm when the GVF was low. The simulation settings are shown in Table 3.

Table 3 Simulation Settings of the twin-screw multiphase pump

Items	Settings
Inlet and outlet boundary	Opening
Reference pressure	1atm
Turbulence model (liquid phase)	SST k-ω turbulence model
Turbulence model (gas phase)	Disperse zero equation
Working medium	Water and air

Inlet turbulence intensity	5%
Multiphase flow model	Euler-Euler heterogeneous flow model
Interphase area transfer model	Particle model.
Bubble diameter	0.2mm
Mesh movement control	Junction box with Fortran
Wall surface	Non-slip boundary conditions

3. Experiment and model validation

3.1 Test platform

As shown in Fig. 4, a performance testing platform for the twin-screw multiphase pump was designed and built to test its performance and verify the numerical model according to the standard JB/T12752-2015[26]. The flow chart is shown in Fig. 5. There are water and gas channels on the test bench. The inlet pressure of the twin-screw multiphase pump is controlled by the liquid pump and the stop valve. The pressure sensors, temperature sensors, liquid flow meters were equipped on the pipe. The gas supply system includes an air compressor, drying machine, gas filter, gas mass flow meters(50L/min、250L/min), pressure and temperature sensors. The gas enters the gas-liquid mixer to mix with the water.

Fig. 4 Performance testing platform of twin-screw multiphase pumps

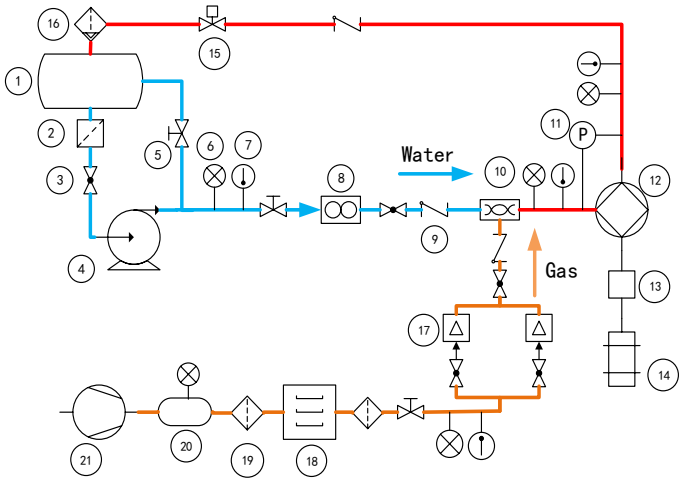

1.Water storage tank; 2.Liquid filter; 3.Ball valve; 4.Liquid pump; 5.Stop valve; 6.Pressure sensor; 7.Temperature sensor; 8.Liquid flow meter; 9.Check valve; 10.Gas-liquid mixer; 11.Differential pressure transmitter; 12.Twin-screw multiphase pump; 13.Torque meter; 14.Variable frequency motor; 15.Electrically operated valve; 16.Gas-liquid separator, 17.Gas mass flow meter(50ml、250ml); 18.Drying machine; 19.Gas filter; 20.Air storage tank; 21.Air compressor

Fig. 5 The flow chart of the testing platform

Table 4 shows the range and accuracy of the sensors and the equipment. Absolute errors of flow rate, power, volumetric efficiency, and hydraulic efficiency could be calculated according to the accuracy grade of equipment and transfer error equations[27]. The absolute errors were represented by error bars in data graphs.

Table 4 Range and accuracy of the equipment

Equipment Name	Range or performance parameter	Accuracy grade
Liquid flow meter	4.0MPa, 15m/s	0.5

Gas mass flow meter	0-50SLPM, 0-250SLPM	1
Twin-screw multiphase pump	0-0.8MPa, 1450r/min, 15m^3/h	
Torque meter	0-100	0.2
Pressure sensor	0-0.8MPa, 0-1MPa	0.075
Differential pressure transmitter	0-1.2MPa	0.075

Table 5 shows the test conditions. The experiments were done under different IGVF.

Table 5 Test conditions of the twin-screw multiphase pump

Working condition	Inlet pressure /MPa	Rotate speed /r·min^{-1}	Outlet pressure /MPa	IGVF /%
Multiphase transportation	0.1	1450	0.8	0, 2.5, 5.0, 7.5, 10

3.2 The experiment and model validation

Figure 6 shows the flow rate and power curves of the twin-screw multiphase pump under different IGVF. It can be seen that the test flow rate experiment is less than the simulation value. With the increase of IGVF, the flow rate of the twin-screw multiphase pump decreases. The deviations between the experiment and simulation results are small, and the maximum deviation is 3.2% at 10% IGVF. At low IGVF, the gas will be uniformly dispersed into the liquid, resulting in the decrease of the viscosity of the gas-liquid mixture. Hence, the leakage at the pump gaps increases, which leads to the decrease of the volume flow rate. The power does not change significantly with the increase of IGVF. The maximum deviation between the simulation and experiment power is 2.4% at the IGVF of 0.

Figure 7 shows the hydraulic and volumetric efficiency curves of the twin-screw multiphase pump under different IGVF. When the IGVF increases from 0% to 10%, the twin-screw multiphase pump's hydraulic and volumetric efficiency decrease slightly, caused by the volume flow rate decrease. The maximum deviations between simulation and experiment results for hydraulic and volumetric efficiency are 1.7% and 3.2%. Both of the maximum deviations occur at the IGVF of 10%. Therefore, the overall deviation between simulation and experiment data is low, and the numerical simulation model is verified basically.

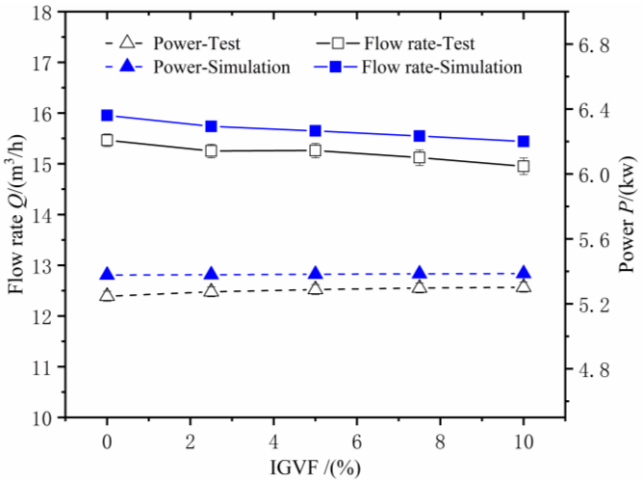

Fig. 6 Curve of flow rate and power of the twin-screw multiphase pump under different IGVF

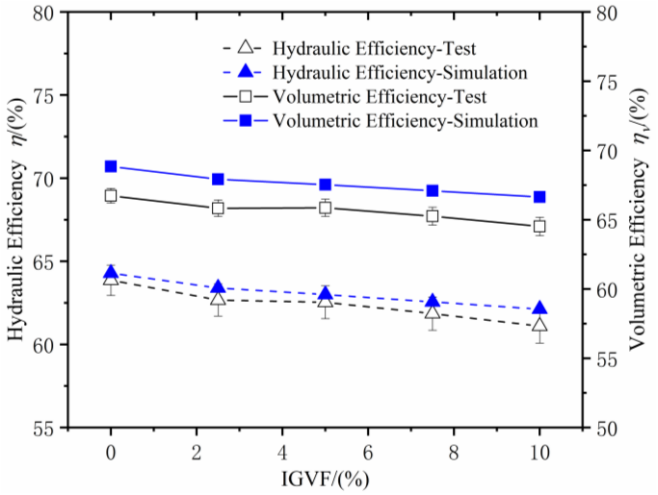

Fig. 7 Curve of hydraulic and volumetric efficiency of the twin-screw multiphase pump under different IGVF

4. Numerical simulation results and analysis

4.1 Pressure distribution

Figure 8(a) shows the pressure distribution in the working chambers when the IGVF is 10%. The pressure in each working chamber of the twin-screw multiphase pump is uniform. The pressure difference exists between two adjacent working chambers.

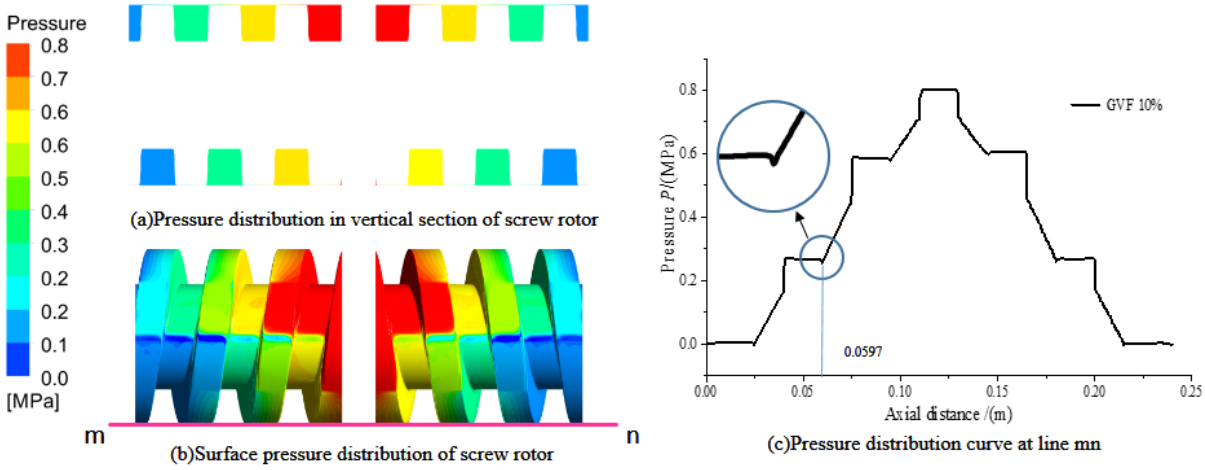

Fig. 8 Pressure distribution in the pumps under 10% IGVF

Figure 8(b) shows the pressure distribution on the surface of the screw rotors. At the inlet of the twin-screw multiphase pump, the pressure is lower than 0.1 MPa. The pump accelerates the suction fluid. As the velocity increases, the static pressure decreases. The same phenomenon also occurs at the gap. When the working fluid flows through the gap, a jet generates under the pressure difference between the upstream and downstream, which results in the drop of local static pressure. Because the numerical model did not include the cavitation model, the local static pressure reaches 0. Fig. 8(c) shows the pressure distribution along the purple line mn labeled in Fig. 8(b). It can be seen that the pressure variation in working chambers is very slight. At the entrance of the tip gap from the high-pressure chamber to the low-pressure chamber, the pressure drops sharply. Then, the pressure decreases linearly along the tooth tip gap. At the exit of the tip gap, the pressure curve has a small trough due to the leakage jet. From the two ends of the screw to the middle, the pressure increases step by step and is symmetrical from left to right. Therefore, the axial force of the twin-screw multiphase pump can be balanced by itself.

4.2 GVF distribution

Figure 9 shows the GVF distribution in the working chamber at 10% IGVF. The gas distribution is uneven in the working chamber, and there are high GVF accumulation areas in every working chamber. The high GVF areas scatter and are not concentrated near the root of the rotors, which deviates from the assumption in references[4,5]. The reason is that the bubble size in the simulation was set to be 0.2mm. The small gas bubble moved with the turbulent liquid flow quickly. From the enlarged view in Fig. 9, the two-phase leakage flow is laminar in the tooth tip gap, where the maximum Reynolds number is 1114. The liquid is on the top due to the centrifugal force, while the gas concentrates on the bottom.

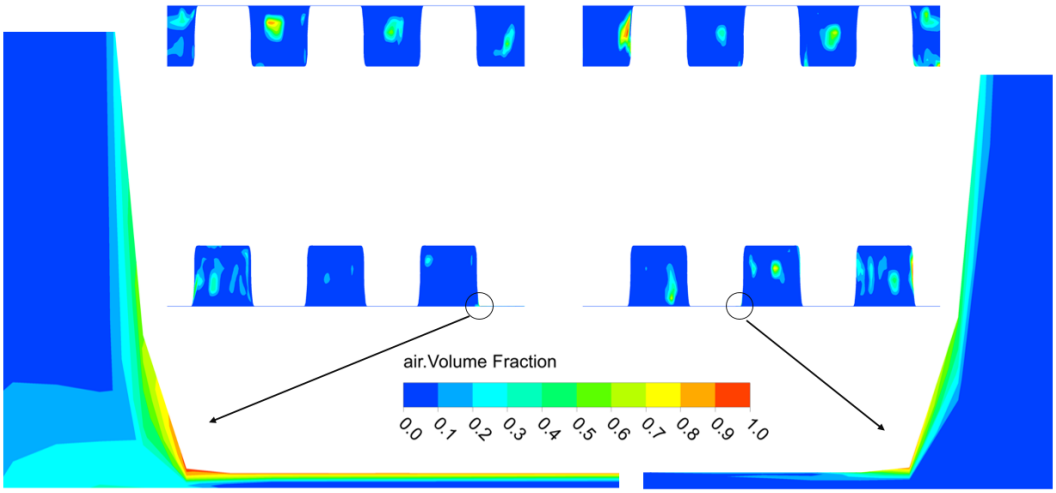

Fig. 9 GVF distribution on the horizontal section at 10% IGVF

Figure 10 shows the GVF distribution at four different heights in the discharge pipe. Y is the distance between the position of Cut-view and the horizontal center plane. The position of Y=0 locates at the horizontal center surface of the rotors in Fig. 3. The GVF distribution in the discharge pipe was affected by the discharge flow in the discharge chamber. First, the two-phase flow flows out from the last working chamber to the discharge chamber. Then, the two-phase flow turns 90° and flows into the discharge pipe. Finally, affected by the centrifugal force, the liquid phase is delivered to the center of the discharge pipe while the gas accumulates near the

pipe wall, as shown in the figure of Y=150mm of Fig. 10. Thus, there are four high GVF areas as four jet flow exists in the discharge chamber. It can be seen that four high GVF areas move to the center of the pipe as the Y value increases.

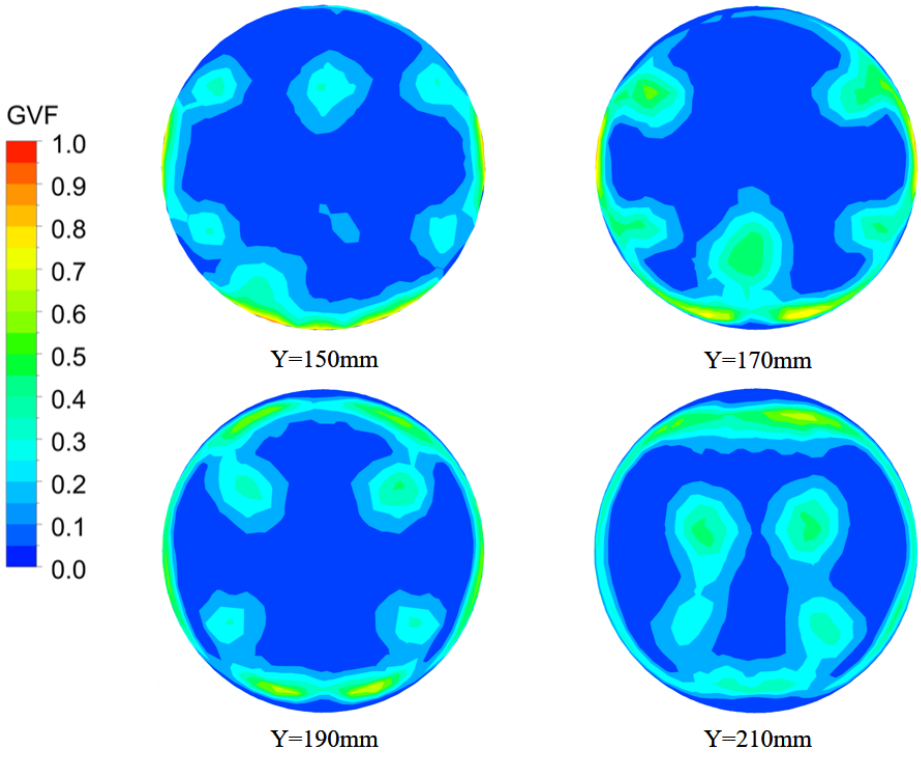

Fig. 10 GVF distribution in discharge pipe at 10% IGVF

4.3 Velocity field

Figure 11 shows the contour of the water velocity of the horizontal section at the IGVF of 10%. The water velocity in the working chamber is much lower than that at the leakage gap. Furthermore, there exists the velocity gradient from the wall to the center of the chamber. There are two reasons for the phenomena. One is the rotor surface velocity, which drives the fluid in working chambers to move. The other is the high-speed leakage flow near the gaps, which causes the local high velocity near the inlet and outlet of the gap. An enlarged view of the velocity field in the tip gap is also provided. The maximum velocity is at the center of the tip gap.

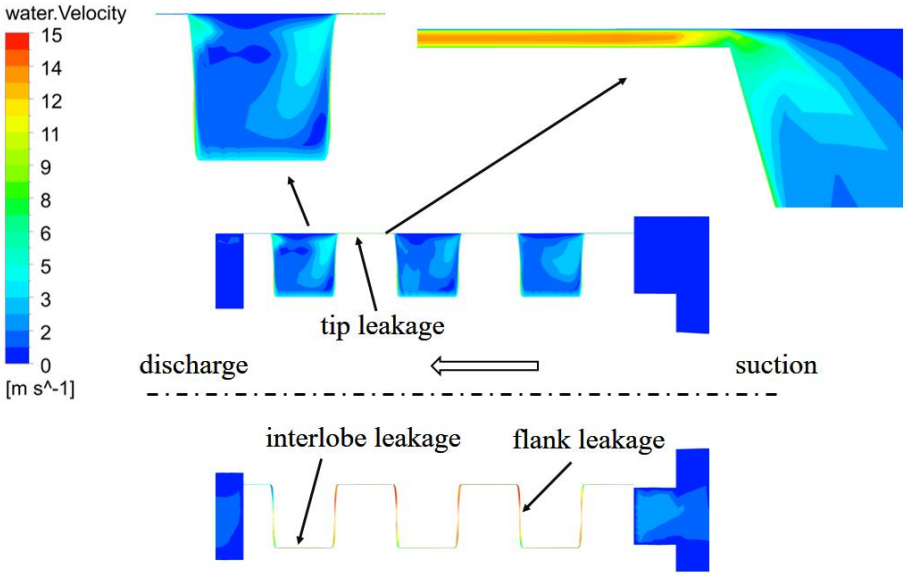

Fig. 11 Contour of water velocity on the horizontal section at 10% IGVF

As shown in Fig. 11, there are three kinds of leakage: tip leakage, interblobe leakage, and flank leakage. The 3D leakage velocity vectors at different cross-sections of the rotors are shown in Fig. 12. The tip leakage velocity is vertical to the cross-section, and its value is almost unchanged. The interlobe leakage occurs in the gap between the tip and root of the rotors. The velocity of the interlobe leakage is the largest. The maximum velocity appears at the second cross-section and reaches 35m/s. The flank leakage happens at the tooth side of the rotors.

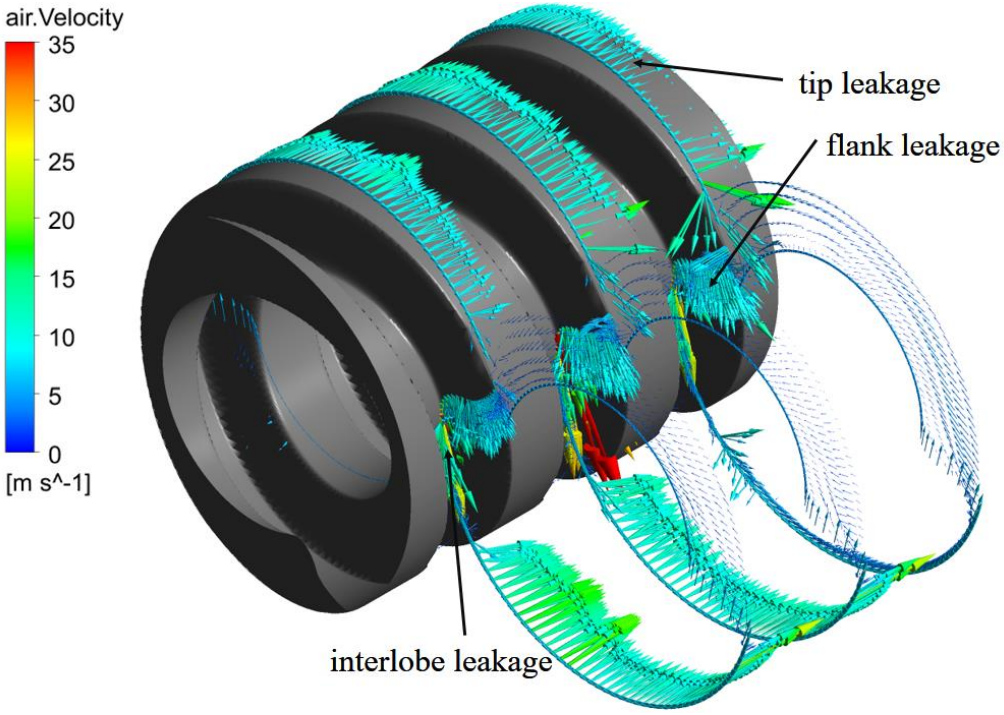

Fig. 12 The gas velocity vector at three different cross-sections at 10% IGVF

Figure 13 shows the water velocity vector of the outlet section at Y=150mm and Y=190mm at 10% IGVF. There are four vortices inside the discharge pipe, and the locations of vortices are the same as that of the high GVF areas inside the discharge pipe at 10% IGVF in Fig. 10. The vortices are caused by the jet flow from the last working chamber when the last working chamber is open to the discharge chamber. When the multiphase pump runs for a cycle, the working chamber of the male and female rotors connects with the discharge chamber alternatively, which results in four jet flows. The jet flows provide the horizontal vorticity and cause four vortices in Fig. 13. The vortices will transfer gas from the edge to its center. So, the vortex position almost coincides with the position of the high GVF area, as shown in Fig. 10.

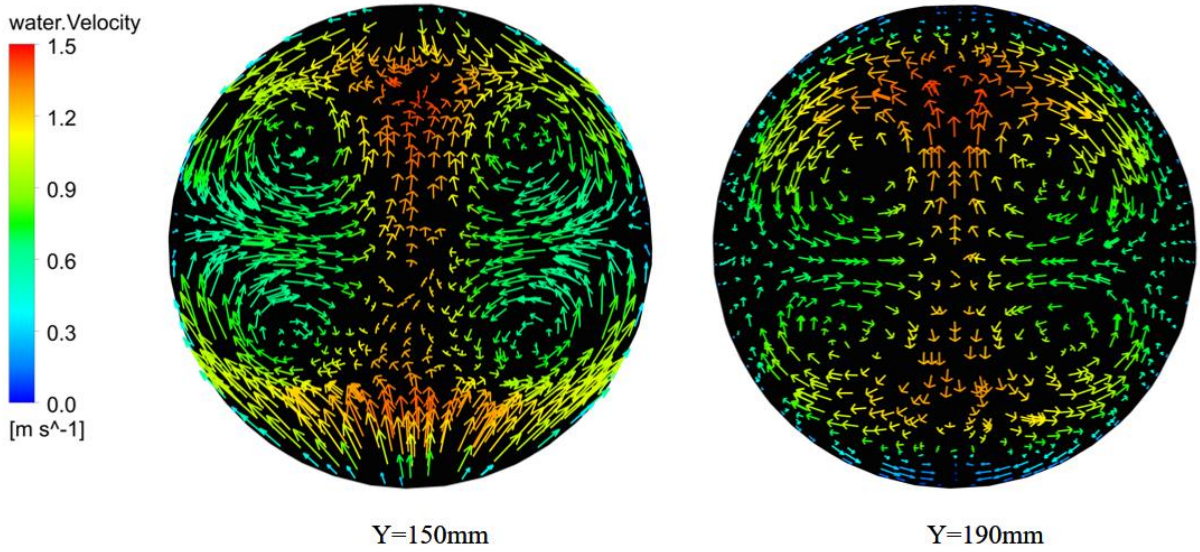

Fig. 13 Liquid velocity vectors at two cross-sections at 10% IGVF in the discharge pipe

5. Conclusion

The numerical model of the twin-screw multiphase pump was established and validated in this paper firstly. Then, the flow characteristics and flow field distribution of the twin-screw multiphase pump were analyzed and studied at 10% IGVF. The main conclusions are summarized as follows:

(1) The numerical simulation model is verified by the experiment. The flow rate, power, hydraulic efficiency, and volumetric efficiency deviations between experiment and simulation results are low, and the maximum deviation is 3.2% at 10% IGVF.

(2) The pressure in each working chamber of the pump is uniform. However, from the high-pressure to the low-pressure chamber, the pressure drops sharply at the entrance of the tip gap and then decreases linearly along the gap.

(3) The GVF distribution is uneven in the working chamber. The two-phase leakage flow in the tooth tip gap is laminar, where the liquid is on the top, and the gas is at the bottom.

(4) Four horizontal vortices happen in the discharge pipe caused by the discharge jet flow when the last working chamber connects with the discharge chamber. As the Y value increases, the gas and the high GVF areas gradually move to the center of the vortices

(5) The water velocity at the gaps is higher than that in the working chamber. The interlobe leakage velocity is the largest. The maximum velocity appears at the second cross-section and reaches 35m/s.

Acknowledgments

This work was supported by the National Natural Science Foundation of China (51839010), Joint Fund Project of Shaanxi Province (2021JLM-55, 2019JLP-25), National Science and Technology Key Laboratory Stability Support Project (614221720180204), Shaanxi University Youth Innovation Team(2020-29), and Centre for compressor technology at City, University of London. The supports are gratefully acknowledged.

References

[1] Anwar, Zeeshan., 2017, "Subsea Technology Multiphase Pumping," SPE/IATMI Asia Pacific Oil and Gas Conference and Exhibition, Jakarta, Indonesia, SPE-186232-MS.

[2] Yu Yiquan, 2018, "Research and application of twin-screw oil-gas mixed pump for deep-sea oil production," Industrial Engineering, Vol. 9, No. 2, pp. 147-149. (in Chinese)

[3] Li Huaiyin, Dang Xuebo, 2016, "Application Research of Subsea Technologies in Deep Water Oil/Gas Field," China Petroleum Machinery, Vol. 44, No. 10, pp. 52-58. (in Chinese)

[4] Vetter G, Wirth W, Korner H, et al., 1999, "Multiphase Pumping with Twin-Screw Pumps Understand and Model Hydrodynamics and Hydro Abrasive Wear," The 17th International Pump Users Symposium, Houston.

[5] PRANG A J, COOPER P., 2004, "Enhanced multiphase flow predictions in twin-screw pumps," 21st International Pump Users Symposium, Baltimore, USA.

[6] Feng C, Yueyuan P, Ziwen X, et al., 2001, "Thermodynamic performance simulation of a twin-screw multiphase pump," Proceedings of the Institution of Mechanical Engineers, Part E: Journal of Process Mechanical Engineering, Vol. 215, No. 2, pp. 157-163.

[7] Hu B, Cao F, Yang X, et al., 2016, "Theoretical and experimental study on conveying behavior of a twin-screw multiphase pump," Proceedings of the Institution of Mechanical Engineers, Part E: Journal of Process Mechanical Engineering, Vol. 230, No. 4, pp. 304-315.

[8] K. Räbiger, T.M.A Maksoud, J Ward, et al., 2008, "Theoretical and experimental analysis of a multiphase screw pump, handling gas-liquid mixtures with very high gas volume fractions," Experimental Thermal & Fluid Science, Vol. 32, No. 8, pp. 1694-1701.

[9] Zhang Yuanxun, Tang Qian, Li Zhonghua, 2014, "Leakage mechanism of screw pump based on leakage model in fluid mechanics," Transactions of the Chinese Society for Agricultural Machinery, Vol. 45, No. 10, pp. 326-332, 339. (in Chinese)

[10] Liu P, Patil A, Morrison G., 2017, "Multiphase Flow Performance Prediction Model for Twin-Screw Pump," Journal of Fluids Engineering, Vol. 140, No. 3, pp. 031103.

[11] Shive J. S., "2017 Leakage Flow Modeling for Multiphase Twin-Screw Pumps" Ph. D. Thesis, Texas: Texas A&M University.

[12] Sina Y, Xingqi L, Jianjun F, et al., 2019, "Numerical Simulation of a Gas-Liquid Centrifugal Pump under Different Inlet Gas Volume Fraction Conditions," International Journal of Fluid Machinery and Systems, Vol. 12, No. 1, pp. 56-63.

[13] Rane S, Kovacevic A., 2017, "Algebraic generation of single domain computational grid for twin screw machines. Part I. Implementation," Advances in Engineering Software, Vol. 107, pp. 38-50.

[14] Kovacevic A, Rane S., 2017, "Algebraic generation of single domain computational grid for twin screw machines Part II–Validation," Advances in Engineering Software, Vol. 109, pp. 31-43.

[15] Yan D, Tang Q, Kovacevic A, et al., 2017, "Rotor profile design and numerical analysis of 2-3 type multiphase twin-screw pumps," Proceedings of the Institution of Mechanical Engineers, Part E: Journal of Process Mechanical Engineering, Vol. 232, No. 2, pp. 186-202.

[16] Yan D, Kovacevic A, Tang Q, et al., 2017, "Numerical investigation of cavitation in twin-screw pumps," Proceedings of the Institution of Mechanical Engineers, Part C: Journal of Mechanical Engineering Science, Vol. 232, No. 20, pp. 3733-3750.

[17] Yan D, Kovacevic A, Tang Q, et al., 2016, "Numerical modelling of twin-screw pumps based on computational fluid dynamics," Proceedings of the Institution of Mechanical Engineers, Part C: Journal of Mechanical Engineering Science, Vol. 231, No. 24, pp. 4617-4634.

[18] ZHANG Linghong, LIU Ruiqing, WANG Jun, et al., 2018, "Investigation on flow field characteristics of double-tooth full-smooth screw in twin screw pump," Fluid Machinery, Vol. 46, No. 6, pp. 17-21. (in Chinese)

[19] Zhang D, Cheng L, Li Y, et al., 2020, "The hydraulic performance of twin-screw pump," Journal of Hydrodynamics, Vol. 32, No. 3, pp. 605-615.

[20] Zhang X, Yang J, Bei W, et al., 2021, "Optimal Structure Design and Performance Analysis of Multiphase Twin-screw Pump for Wet Gas Compression," International Journal of Fluid Machinery and Systems, Vol. 14, No. 2, pp. 208-219.

[21] Sun S H, Wu P B, Guo P C, et al., 2021, "Numerical investigation on a double suction twin-screw multiphase pump." IOP Conference Series: Earth and Environmental Science, Vol. 774, No. 1, pp. 012048.

[22] Zhang WB, Jiang QF, Bois G, et al., 2019, "Experimental and Numerical Analysis on Flow Characteristics in a Double Helix Screw Pump," Energies, Vol. 12, No. 18, pp. 3420.

[23] Rane S, Kovačević A, Stošić N., 2015, "Analytical Grid Generation for accurate representation of clearances in CFD for

Screw Machines," British Food Journal, Vol. 90, No. 1, pp. 012008.
[24] N. Stosic, I.K. Smith, A. Kovacevic., 2019, "SCORG Help Manual," PDM Analysis Ltd.
[25] ZHANG Jinya, CAI Shujie, ZHU Hongwu., 2015, "Visualization Test for Flow Field of Gas-liquid Two-phase in the Entrance of Rotodynamic Multiphase Pump," Chinese Journal of Mechanical Engineering, Vol. 51, No. 18, pp. 184-190.
[26] Tianjin Pump & Machinery Group Co. Ltd, 2016, Multiphase twin screw pump, JB/T 12752-2015, China Standard Quality Supervision Press, Beijing. (in Chinese)
[27] Wu Daoti., 2004, Non-electric measurement technology, Xi'an Jiaotong University Press, Xi'an. (in Chinese)